Vibration-Induced Rotation

by

Patrick Andreas Petri

Submitted to the Department of Mechanical Engineering
in partial fulfillment of the requirements for the degree of

Bachelor of Science in Mechanical Engineering

at the

MASSACHUSETTS INSTITUTE OF TECHNOLOGY

[June 2001]
May 2001

Author .....
Department of Mechanical Engineering
May 11, 2001

Certified by .....
Samir A. Nayfeh
Assistant Professor of Mechanical Engineering
Thesis Supervisor

Accepted by .....
Ernest G. Cravalho
Chairman, Undergraduate Thesis Committee

Vibration-Induced Rotation

by

Patrick Andreas Petri

Submitted to the Department of Mechanical Engineering
on May 11, 2001, in partial fulfillment of the
requirements for the degree of
Bachelor of Science in Mechanical Engineering

Abstract

This thesis presents, explores, and documents the validation of a mechanical mechanism dubbed Vibration-Induced Rotation, or VIR. The tendency of threaded fasteners to move under the influence of vibrations is well known, but never before has the root cause been identified and investigated in search of beneficial consequences. The sense of rotation, speed, and force with which a threaded body moves in an appropriately vibrated medium is a function of the excitation. The principal kinematic and dynamic relationships governing VIR have been developed and experimentally affirmed. There is evidence for more complex modes of motion, but pure VIR remains the dominant response under a wide variety of conditions. Simplicity, robustness, and uniqueness suggest a multitude of possible applications, particularly in the areas of product assembly and fastener insertion. This thesis should provide a cornerstone in a new and promising field of application-oriented research.

Thesis Supervisor: Samir A. Nayfeh
Title: Assistant Professor of Mechanical Engineering

Acknowledgments

Many thanks to Professor Samir Nayfeh, who patiently guided me through the thesis creation process without bounding my creativity.

I am also indebted to the Edgerton Student Shop, especially Fred Cote, as well as the Pappalardo Lab, the Lab for Manufacturing and Productivity (LMP), and the Media Lab, for furnishing the tools, parts, and advice required to complete this work.

A thousand thanks to Laura Baldwin of Athena On-Line Consulting (OLC), who patiently spent innumerable hours helping me include graphics and figures in this document.

I would like to acknowledge the support I have received from family, friends, faculty, and others in times that were often stressful and exhausting.

Finally. I would like to thank MIT and the Mechanical Engineering department for giving me the opportunity to undertake such exiting work.

Contents

List of Figures

Chapter 1

Introduction

1.1 A Brief History

In March of 2000, I was working in one of MIT's machine shops, creating a part for our school's FIRST team robot. The part consisted of a motor face-mounted to a mounting bracket by a set of screws, and a spur gear fastened to the motor shaft by means of a set screw. Since the motor shaft interfered with another part, I was compelled to shorten it with a hack saw.

When I started sawing, to my surprise, all the mounting screws steadily unwound themselves from their cavities. Beyond astonishment I felt vexation, since the screws were difficult to reach in their location behind the gear. It also seemed strange that all four screws turned the same way without indecision, since sawing, in my mind, was perfectly symmetric with respect to either sense of rotation. To test the symmetry assumption, I moved to the opposite side of the shaft, and continued sawing. Indeed, all screws scurried back into position! My immediate problem was solved, but my curiosity remained.

Upon a few days' consideration, I reached the conclusion that the critical modes of excitation were two dimensional; specifically, that they must be circular. The right interplay of horizontal shaft deflection and vertical saw bouncing created the required

motions. Due to the asymmetry of the saw blade teeth, these vibrations were only created on the return stroke, explaining the observed characteristics.

In any case, the phenomenon was potentially explained. Since any effect can be used to some advantage, I was intent on testing my theory and exploring the issue further. With a scrap block of aluminum and a toy Radio Shack motor from one of my classes, I created the first VIR device. A nut was taped onto the motor shaft to constitute an eccentric mass. Manually pressing the motor firmly to the block created barely perceptible motions, but undaunted, I machined a hole into the block in which the motor was press fitted. The resulting construction worked successfully!

Seizing the unique opportunity that this discovery offered, I decided to develop the idea as my undergraduate thesis. The results of my work are in your hands.

1.2 Fundamentals

Vibration-Induced Rotation, abbreviated VIR, is a slightly counterintuitive three-dimensional phenomenon. In its purest form, a threaded cylinder is located in a block of some sort, and the block subjected to circular vibrations. More precisely, the block must be excited sinusoidally in both directions orthogonal to the axis of the cylinder, with a significant phase difference between both two motions. If the cylinder rolls without slip inside the hole, it is kinematically constrained to rotate slowly in the opposite direction. Due to its threads, the cylinder will move helically in or out of the block as well. The direction of motion reverses in conjunction with the excitation phase.

1.3 Literature Review

Despite intensive literature searches, no records of the phenomenon of VIR have been found. Extensive studies have been performed on fastener loosening, but none allude to multidimensional excitations. Parts feeders use circular vibrations frequently; how-

ever, the actuated surface is usually flat. Some parts are moved in circular drums, yet never in close confines or high speeds. Several patented piezoelectric actuators convert circular vibrations into rotary motion, but usually through asymmetric geometry involving stick-slip contact, or similar means. To the best of the author's knowledge, no concept remotely resembling VIR has been documented, implemented, or studied.

1.4 Objectives

The intent of this thesis is to present, explain, validate, and explore the concept of VIR. The work presented in this thesis is as theoretical and general as possible, to maximize its breadth of applicability to real-world applications. In a sense, the motivation of this study is to lay the groundwork for feasibility estimates, which any engineer wishing to develop VIR will face before making an informed go/no-go decision.

Physical demonstrations would be much more effective than any written description, but Chapter 1 should give an intuitive idea of what VIR represents. Chapter 2 then derives a theoretical model of the main physical characteristics of any VIR device. These governing equations are compared to experimental results in Chapter 3. In addition, Chapter 3 contains empirical results that are more difficult to model, but remain of immediate interest to potential developers. Finally, Chapter 4 discusses potential applications at a more concrete level, and suggests avenues of further exploration.

1.5 Patent Status

This document will be submitted for provisional patent protection the week of May 14, 2001. To date, extensive literature search suggests broad patentability. If no new conflicting claims are discovered, the MIT Technology Licensing Office will attempt to patent VIR within the upcoming months.

Chapter 2

Theory

2.1 Angular Velocity

A study of the dynamics of a smooth cylinder rolling without slip in a hole casts significant light on the behavior of an actual VIR system. The constraint that threads place on axial motion is easily appended to the model, providing a simplified analytic description of motion.

In another variant of VIR, hereafter referred to as the "inverted" case, an object with internal threads is driven by a threaded rod. If this object is referred to as the "nut," the term should be considered a mnemonic, since the dynamics generalize to any system with similar geometry. Although it is mathematically possible to derive both scenarios from the same model, in the interest of clarity, this paper will treat the two cases independently.

2.1.1 Standard Case

Figure 2-1 depicts the system under consideration. Since the cylinder is tangent to the medium, which may subsequently be referred to as "the block", points B, C, and D must be collinear. Let $\mathbf{v}_{C/B}$ be the velocity of point C relative to point B; that

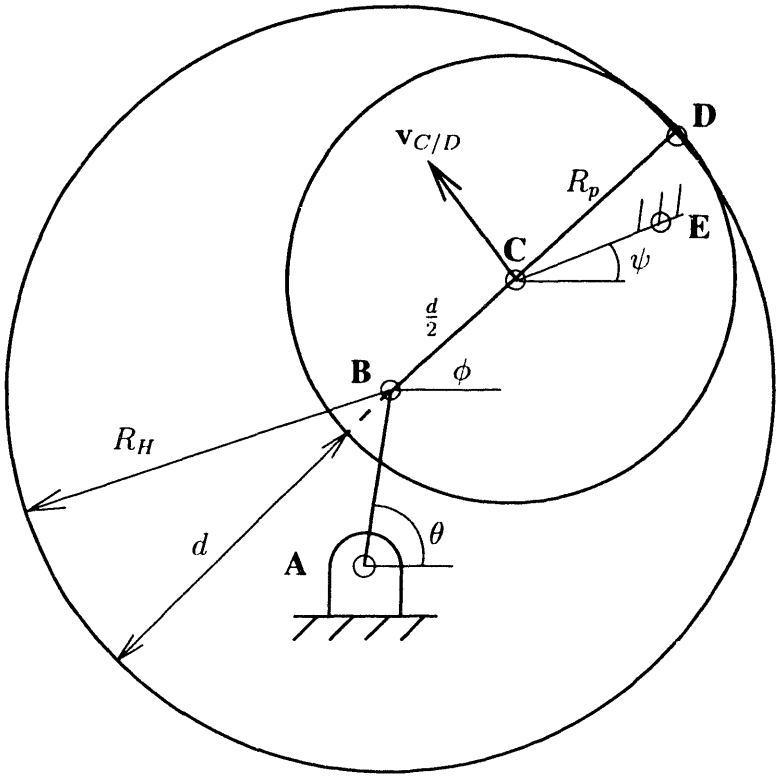

Figure 2-1: Cylinder rolling without slip in a hole

is, the velocity of the center of mass of the cylinder with respect to the block. If d is the play, or gap, between the screw and the block (formally, $d = D_H - D_P$) the separation of points B and C must be $\frac{1}{2}d$. Then the diagram implies that

$$v_{C/B} = \tfrac{1}{2}d\dot{\phi}. \tag{2.1}$$

Let ψ be a measure of the absolute angular orientation of the cylinder. Here, it is shown as the angle between segment $\overline{CE}$ fixed to the cylinder and a stationary horizontal line. Note that θ does not contribute to ψ, since the block itself does *not* rotate. Since B and D are points on the same rigid body,

$$v_{C/B} = -R_p\dot{\psi} \tag{2.2}$$

Combining (2.1) and (2.2), we find

$$\boxed{\dot{\psi} = -\frac{d}{2R_p}\dot{\phi} = -\frac{d}{D_p}\dot{\phi}} \tag{2.3}$$

This is the velocity relationship for a cylinder rolling in its hole.

2.1.2 Inverted Case

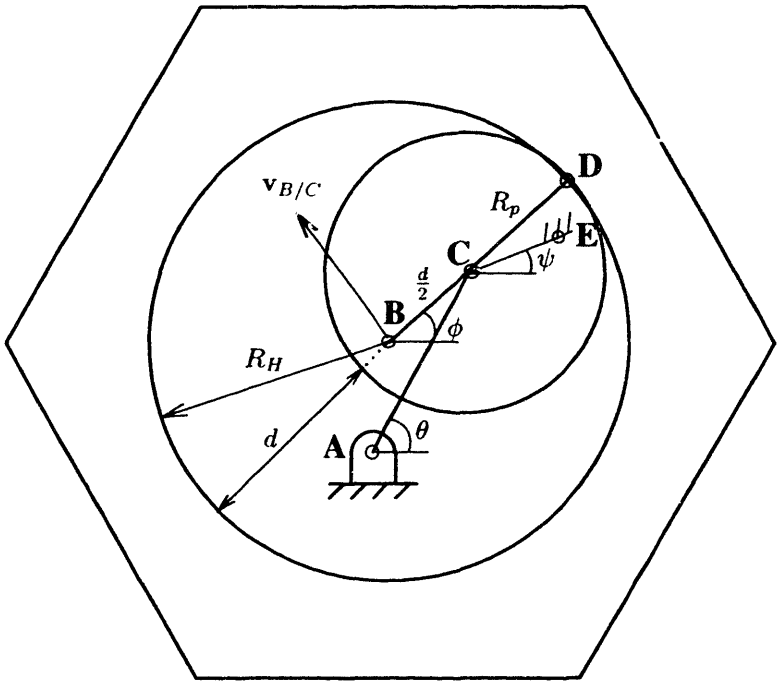

Figure 2-2: Block rolling without slip around a cylinder

In the inverted case, the kinematic driver-follower relationship is inverted. In addition, the velocity of interest is now $\mathbf{v}_{B/C}$, which complicates the change somewhat. Figure 2-2 depicts the slightly altered model. R_H is renamed R_n to reflect the fact that the hole diameter is now the pitch diameter of the internally threaded object.

Using otherwise similar notation,

$$v_{B/C} = -\tfrac{1}{2} d\dot{\phi} \tag{2.4}$$

and

$$v_{B/C} = -R_n \dot{\psi}, \tag{2.5}$$

hence

$$\boxed{\dot{\psi} = \frac{d}{R_n}\dot{\phi} = \frac{d}{D_n}\dot{\phi}}. \tag{2.6}$$

This is the velocity relationship verified in Subsection 3.3.2. The most notable difference is that a nut will rotate in the same direction as its excitation, while a bolt will turn the other way. Otherwise, the standard and inverted frequency reduction relations are very similar, although it is worth noting that the pitch radius of interest, R_n, is now that of the internally threaded body.

2.2 Equation of Motion

Let $\mathbf{R}$ be the position vector locating the center of the screw. In terms of our moving coordinate vectors, whose definitions are sketched in Figure 2-3,

$$\mathbf{R} = a_v\, \hat{\mathbf{a}}_1 + \tfrac{1}{2} d\, \hat{\mathbf{b}}_1 \tag{2.7}$$

Differentiating, we find velocity

$$\dot{\mathbf{R}} = a_v(\dot{\theta}\hat{\mathbf{k}} \times \hat{\mathbf{a}}_1) + \tfrac{1}{2} d(\dot{\phi}\hat{\mathbf{k}} \times \hat{\mathbf{b}}_1) \tag{2.8}$$

$$= a_v \dot{\theta}\hat{\mathbf{a}}_2 + \tfrac{1}{2} d\dot{\phi}\hat{\mathbf{b}}_2 \tag{2.9}$$

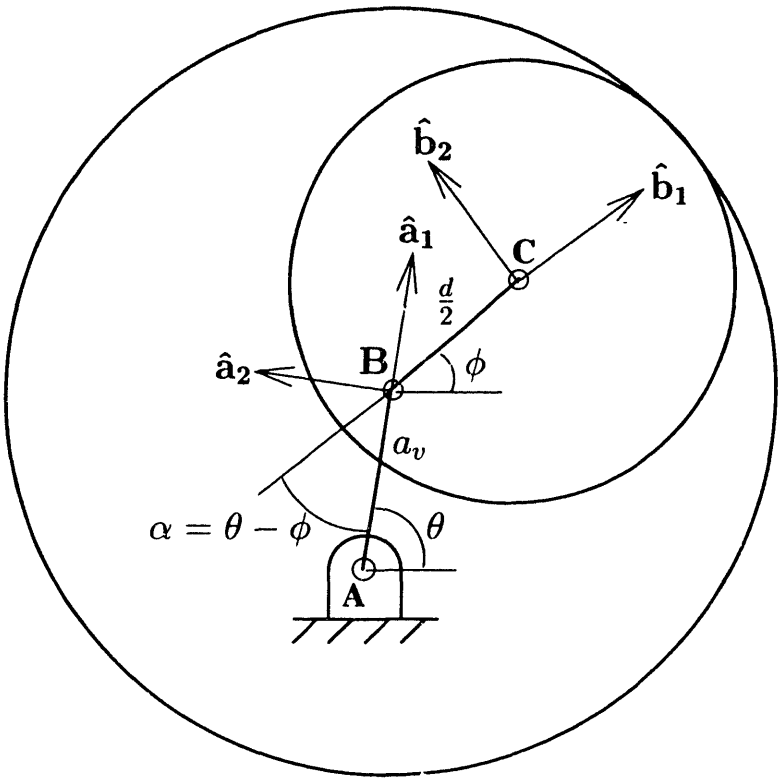

Figure 2-3: Coordinate system setup

Since the driving medium is assumed to undergo uniform circular motion, write $\dot{\theta}$ as ω_v, a constant. Differentiating once again, we obtain

$$\begin{aligned}
\ddot{\mathbf{R}} &= \omega_v \hat{\mathbf{k}} \times (a_v \omega_v \hat{\mathbf{a}}_2) + \dot{\phi}\hat{\mathbf{k}} \times \left(\tfrac{1}{2} d\dot{\phi}\hat{\mathbf{b}}_2\right) + \tfrac{1}{2} d\ddot{\phi}\hat{\mathbf{b}}_2 && (2.10)\\
&= -a_v \omega_v^2 \hat{\mathbf{a}}_1 - \tfrac{1}{2} d\dot{\phi}^2 \hat{\mathbf{b}}_1 + \tfrac{1}{2} d\ddot{\phi}\hat{\mathbf{b}}_2 && (2.11)\\
&= -\left(a_v \omega_v^2 \cos\alpha + \tfrac{1}{2} d\dot{\phi}^2\right)\hat{\mathbf{b}}_1 + \left(-a_v \omega_v^2 \sin\alpha + \tfrac{1}{2} d\ddot{\phi}\right)\hat{\mathbf{b}}_2 && (2.12)
\end{aligned}$$

Figure 2-4 shows the forces acting on our cylinder. Since only the normal force acts in the negative radial direction, while friction provides tangential acceleration, their magnitudes can be inferred directly from the components of $\ddot{\mathbf{R}}$.

$$\boxed{N = m\left(a_v \omega_v^2 \cos\alpha + \tfrac{1}{2} d\dot{\phi}^2\right)} \qquad (2.13)$$

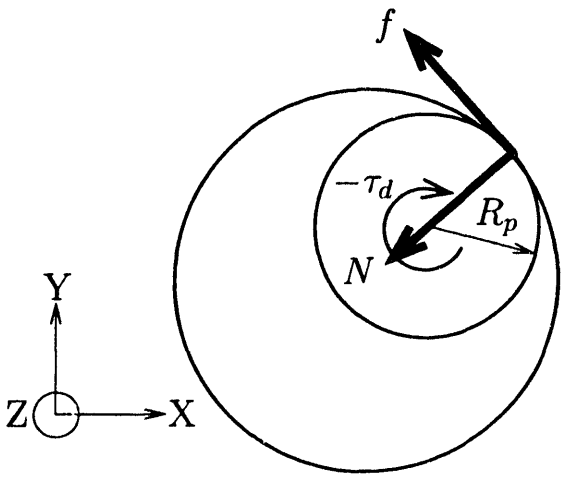

Figure 2-4: Simplified free-body diagram of a bolt

$$\boxed{f = m\left(-a_v\omega_v^2 \sin\alpha + \tfrac{1}{2}d\ddot{\phi}\right)} \tag{2.14}$$

Now consider a torque balance on the cylinder. τ_d is a constant disturbance torque intended to capture the effects of drag, axial load, and other retarding forces.

$$\sum \mathrm{T}_z = I\alpha_z$$

Assuming

$$I = \nu m R_p^2, \tag{2.15}$$

where $\nu \approx \frac{1}{2}$ for a cylindrical bolt,

$$f \cdot R_p + \tau_d = \nu m R_p^2 \ddot{\psi}. \tag{2.16}$$

Using the derivative of (2.3) and rearranging,

$$f + \frac{\tau_d}{R_p} = -\tfrac{1}{2}\nu m d\ddot{\phi} \tag{2.17}$$

Substituting for f from (2.14),

$$\left(\tfrac{1}{2}+\tfrac{1}{2}\nu\right)\ddot{\phi}=\frac{a_v}{d}\omega_v^2\sin\alpha-\frac{\tau_d}{mdR_p} \tag{2.18}$$

Recalling that $\alpha=\theta-\phi$, we find our equation of motion.

$$\boxed{\ddot{\phi}=\frac{2a_v\omega_v^2}{(1+\nu)d}\sin(\theta-\phi)-\frac{2\tau_d}{(1+\nu)mdR_p}} \tag{2.19}$$

To capture the effect of axial inertia, we impose

$$\tau_{d,old}=\tau_d+\tau_{eqv,z} \tag{2.20}$$

Using the principle of virtual work applied to one full rotation of the screw,

$$2\pi\tau_{eqv,z}=lead\cdot F_z \tag{2.21}$$

Let λ be the pitch angle of the screw, usually computed using

$$\tan\lambda=\frac{lead}{2\pi R_p} \tag{2.22}$$

Combining (2.21) and (2.22), we find the transmission ratio.

$$\tau_{eqv,z}=R_p\tan\lambda F_z \tag{2.23}$$

F_z is a fictitious force embodying axial inertia, so

$$F_z=-ma_z \tag{2.24}$$

where a_z must relate to $\ddot{\phi}$ by the inverse of the transmission ratio:

$$a_z = R_p \tan\lambda \, \ddot{\psi} \tag{2.25}$$

By combining (2.20) with (2.23) through (2.25),

$$\tau_{d,old} = \tau_d - mR_p^2 \tan^2\lambda \, \ddot{\psi} \tag{2.26}$$

Substituting the new τ_d into (2.18) and eliminating ψ in favor of ϕ with (2.3),

$$\left(\tfrac{1}{2} + \tfrac{1}{2}\nu\right)\ddot{\phi} = \frac{a_v}{d}\omega_v^2 \sin\alpha - \frac{\tau_d}{mdR_p} - \tfrac{1}{2}\tan^2\lambda \, \ddot{\phi} \tag{2.27}$$

$$\tfrac{1}{2}\left(1 + \nu + \tan^2\lambda\right)\ddot{\phi} = \frac{a_v}{d}\omega_v^2 \sin\alpha - \frac{\tau_d}{mdR_p} \tag{2.28}$$

Hence the equivalent inertial parameter ν_{eqv} must be

$$\nu_{eqv} = \nu + \tan^2\lambda \tag{2.29}$$

The adjustment will typically be on the order of 0.53% for a standard coarse thread, or 0.27% for UNF fasteners, which is clearly negligible in light of other approximations. If such a level of accuracy is actually necessary, it is advisable to find the true moment of inertia for the appropriate bolt, one that accounts for the bolt head, thread dimensions, end taper, and other geometry, and compute the appropriate ν using

$$\nu_{exact} = I_{exact}/(mR_p^2) \tag{2.30}$$

The nut, in the inverted case, obeys very similar equations. From Figure 2-5 it is apparent that

$$\mathbf{R} = a_v \hat{\mathbf{a}}_1 - \tfrac{1}{2} d \, \hat{\mathbf{b}}_1 \tag{2.31}$$

This is identical to (2.7). with the implicit understanding that d is redefined to be

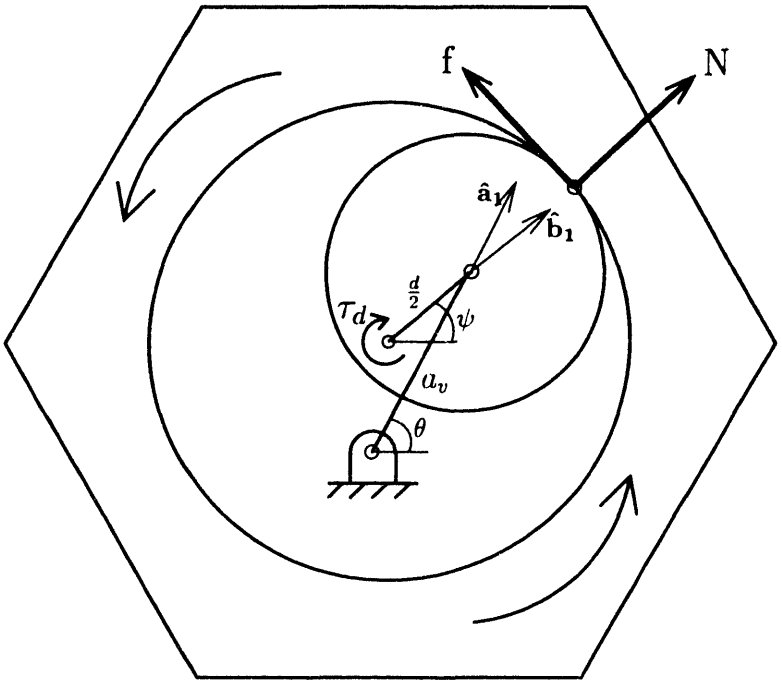

Figure 2-5: Free-body diagram of a nut

$D_n - D_p$, and the standard case derivation is valid to at least (2.14), with

$$f = m\left(-a_v\dot{\theta}^2\sin\alpha - \tfrac{1}{2}d\ddot{\phi}\right) \tag{2.32}$$

Choosing the nut pitch radius R_n as the characteristic length, the analogous force balance to (2.16) is

$$f \cdot R_n + \tau_d = \nu m R_n^2\,\ddot{\psi} \tag{2.33}$$

From the last two equations and the derivative of (2.6),

$$\tfrac{1}{2}\nu m R_n d\ddot{\phi} = -mR_n a_v\omega_v^2\sin\alpha - \tfrac{1}{2}md\ddot{\phi} - \tau_d \tag{2.34}$$

$$-\tfrac{1}{2}(1+\nu)\ddot{\phi} = \frac{a_v}{d}\omega_v^2\sin\alpha + \frac{\tau_d}{mdR_p} \tag{2.35}$$

$$\ddot{\phi} = \frac{-2a_v\omega_v^2}{(1+\nu)d}\sin(\theta-\phi) - \frac{2\tau_d}{(1+\nu)mdR_p} \tag{2.36}$$

In fact, (2.36) could have been derived directly from (2.19) by appropriately substituting for d, reversing τ_d, and renaming R_p.

For a thick-walled hollow cylinder,

$$I = 1/2m(R_{outer}^2 - R_p^2) \tag{2.37}$$

For a typical nut, R_{outer}, the equivalent outer radius, is slightly over twice R_p, the pitch radius. Any ANSI chart will confirm that

$$R_{outer} \approx 2.08R_p \tag{2.38}$$

which gives

$$\nu_{nut} \approx 1/2 * (2.08^2 - 1) = 1.67. \tag{2.39}$$

Again, the equations of motion are sensitive to many factors, so this value should be considered a rough first-order approximation.

2.3 Torques

The amount of resistance a bolt or nut can overcome is a practical concern for almost any VIR device. Unfortunately, an exact prediction is beyond the scope of an undergraduate thesis, for reasons to be discussed at the end of this section. However, an upper bound estimate follows directly from statics.

Since the gap does not appear in the equation of motion, the fact that a bolt would typically start from a centered position appears to have no relevance. If d is exactly zero, our equation would fail by singularity, but any infinitesimal displacement from the center would allow the bolt to break free at the appropriate input phase.

Now, for a bolt to break free, its angular acceleration must be positive. Requiring

$$\ddot{\varphi} = 0 \tag{2.40}$$

yields the promised upper-bound estimate.

$$a_v \omega_v^2 \sin\alpha - \frac{\tau_{d,max}}{mR_p} = 0 \tag{2.41}$$

$$\tau_{d,max} = m a_v \omega_v^2 R_p \sin\alpha \tag{2.42}$$

The phase lag is constrained by friction:

$$f \leq \mu N \tag{2.43}$$

When the bolt is at rest, (2.13) and (2.14) become

$$N = m a_v \omega_v^2 \cos\alpha \tag{2.44}$$

$$f = -m a_v \omega_v^2 \sin\alpha \tag{2.45}$$

Our inequality now reads

$$\tan(-\alpha) \leq \mu \tag{2.46}$$

The triangle constructed in Figure 2-6 elucidates the constrains on α. By definition of the sine function and use of the geometry just described,

$$\boxed{\tau_{d,max} = \frac{\mu m a_v \omega_v^2 R_p}{\sqrt{1+\mu^2}}} \tag{2.47}$$

If a pure axial force retards the bolt, we can use (2.23) to approximate the equi-

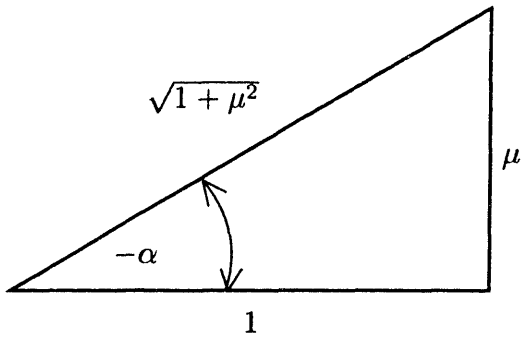

Figure 2-6: Triangle relating μ and α

valent maximum axial load.

$$\boxed{F_{z,max} = \frac{\mu m a_v \omega_v^2}{\tan\lambda\sqrt{1+\mu^2}}} \tag{2.48}$$

Due to the thread angle, a bolt can sustain quite a significant load in steady state. Still, $\tau_{d,max}$ will be significantly smaller experimentally, since angular acceleration must be sufficient to bring the bolt up to speed before α falls into an adverse regime. In addition, a number of factors, including tangential motion, 3-D geometry, the exact nature of the excitation, and the necessity of initially sliding up the thread angle β have been ignored in this model. Nevertheless, (2.47) provides a benchmark by which feasibility may be assessed.

2.4 Dynamic Considerations

So far, all derivations have relied on static models involving either rest or steady state. This section offers some qualitative insights into the dynamical response of VIR systems.

Since ω_v is a constant,

$$\ddot{\alpha} = -\ddot{\phi} \tag{2.49}$$

allowing a convenient change of variable in the equation of motion.

$$\ddot{\alpha} = -\frac{2a_v\omega_v^2}{d(1+\nu)}\sin\alpha + \frac{2\tau_d}{mdR_p} \tag{2.50}$$

Substituting appropriately, we may write for convenience

$$\ddot{\alpha} = -a_v'\sin\alpha + \tau_d' \tag{2.51}$$

$$N = m'\cos\alpha + \tfrac{1}{2}md(\omega_v - \dot{\alpha})^2 \geq 0 \tag{2.52}$$

$$f = -m'\sin\alpha + \tfrac{1}{2}md\ddot{\alpha} \leq \mu N \tag{2.53}$$

Equation (2.51) alone does not imply that steady state is reached, even in the absence of a disturbance. By symmetry, $\sin\alpha$ provides no systematic bias to $\ddot{\alpha}$. However, (2.53) rearranges to

$$\ddot{\alpha} \leq \frac{2\mu}{m}N + \frac{2m'}{m}\sin\alpha \tag{2.54}$$

During startup, whenever (2.51) predicts positive accelerations, the cylinder would actually lose contact. (Since $\alpha = \theta - \phi$, start from rest implies $\dot{\alpha}_o = \omega_v$, so attaining steady state requires negative acceleration in α space.) The nonnegative constraint on N ensures that accelerations are strictly negative at startup. For larger speeds, centrifugal forces cause N to rise, reducing the bias. However, the limitations imposed by the coefficient of friction extend the regime of negative acceleration. Figure 2-7 qualitatively illustrates this scenario. Section 2.5 discusses the effects of loss of contact.

Finite amplitude disturbances about the equilibrium will result in sinusoidal α motion. Viscous drag or its equivalent would dampen the superimposed oscillation, while necessitating a steady state phase lag. This assumption should be appropriate as long as Coulomb friction between cylinder and wall is able to provide the forces dictated by (2.19).

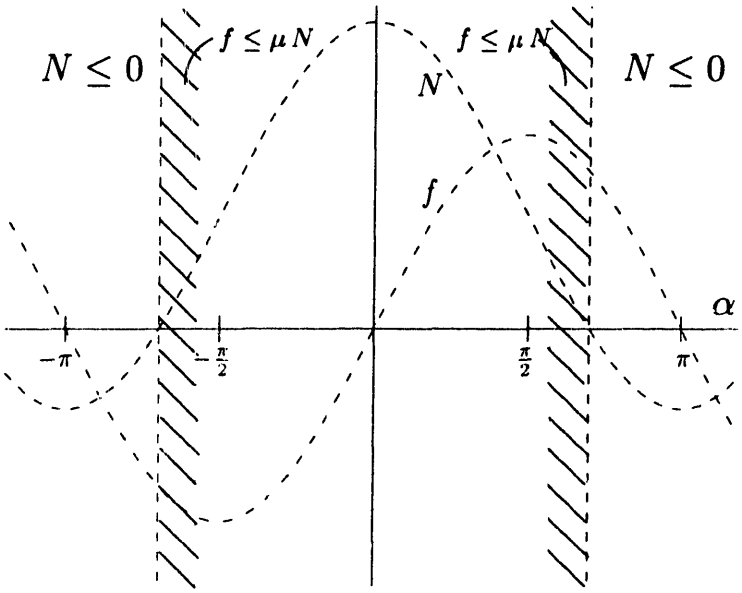

Figure 2-7: α-dependent parameters and their interrelations

2.5 High Frequency/Low Amplitude

Although it has only been mentioned peripherally in Section 2.4, loss of contact with the screw wall may, under some conditions, dominate the dynamics in question. For high-frequency, low-amplitude systems, the path to steady state, if one is ever reached, involves hundreds of disordered collisions between the cylinder and the block, or nut and rod. Even slower systems with amplitudes comparable to the screw gap have been observed to rattle quite loudly, indicating that motion is not smooth, but dominated by a series of collisions.

It may be possible to develop a complete dynamical model of these interactions, but the following arguments should suffice in capturing the salient features of such behavior.

Since the amplitude of vibration is typically smaller than the gap, and orders of magnitude less than the pitch diameter, the situation can be abstracted as depicted in Figure 2-8: a circle approaching a wall with zero curvature. Because the system is radially similar, the approach must be perpendicular to the initial point of contact.

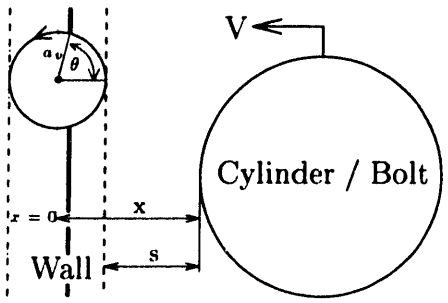

Figure 2-8: Schematic of a cylinder approaching a vibrating wall

The wall vibrates in a perfect circle, yet it is far from equally likely to hit the approaching body during any phase of its motion. This is because the bolt always approaches the boundary from the inside (vice-versa for a nut). To even reach the far side of the vibration cycle, the bolt or nut must already possess considerable speed.

It is clear from the figure that the separation between wall and object is

$$s = x - a_v \cos\theta \tag{2.55}$$

Between collisions, the bolt only contacts the air, which is unlikely to exert significant forces. Hence it should be perfectly reasonable to assume that it moves at constant velocity v.

$$x = x_o - vt \tag{2.56}$$

So

$$s = x_o - vt - a_v \cos\theta \tag{2.57}$$

Figure 2-9 illustrates graphically how a low speed, which represents a shallow slope of approach, renders it impossible to collide anywhere but near the tips of the crests. A typical trajectory T would be associated with a collision favorable to positive spin. Only the trajectory with slope v_{crit} has the minimum speed that will even permit contact in the region $\{\theta \geq -\frac{\pi}{2}\} \cup \{\theta \geq \frac{\pi}{2}\}$, and lose angular speed after contact.

However, to attain such a speed, the bolt in question, assuming that it starts from

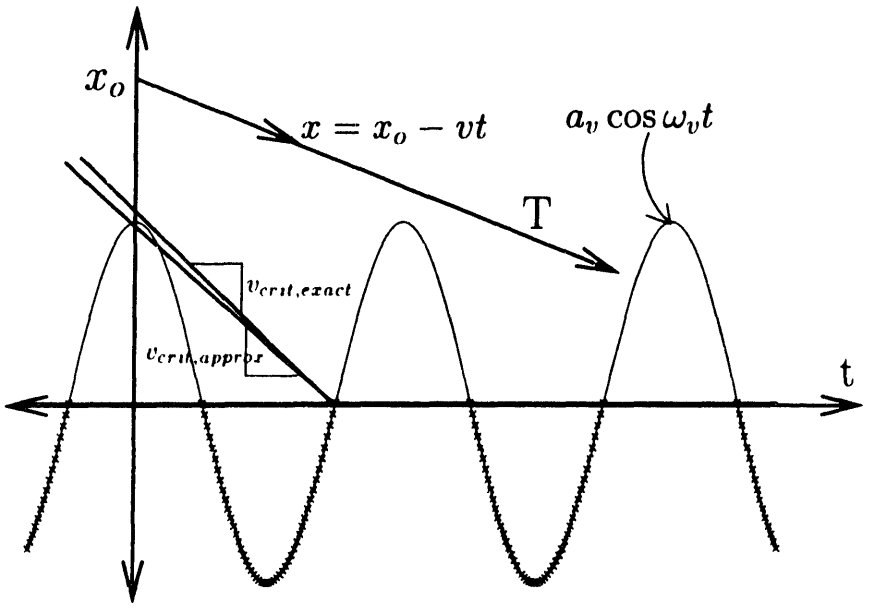

Figure 2-9: Time trajectories of cylinder and wall

rest, must have accumulated noticeable angular momentum. This observation can even be quantified based on the following considerations. Any contact force can be resolved into a horizontal and a vertical component. If collisions are perfectly elastic, the horizontal component does not add energy to the system; if there is inelasticity, energy is lost. On the other hand, the vertical component of the contact force, constituted by friction between the wall and the cylinder, either adds or subtracts translational kinetic energy. Either type of collision will add rotational energy, unless the far side of the vibratory cycle is reached. Generously assuming that translational energy is always added, and never subtracted, the two energies will satisfy the following relation:

$$dE_{translational} = F\delta x \tag{2.58}$$

$$dE_{rotational} = \tau\delta\theta = FR_p \cdot \frac{\delta x}{R_p} = F\delta x \tag{2.59}$$

$$dE_{translational} = dE_{rotational} \tag{2.60}$$

As mentioned, rotational energy will also be bigger, in all likelihood. Upon integra-

tion:

$$E_{translational} \leq E_{rotational} \tag{2.61}$$

$$\tfrac{1}{2} I \dot{\psi}^2 \geq \tfrac{1}{2} m v^2 \tag{2.62}$$

$$\dot{\psi} \geq v\sqrt{\frac{m}{I}} \tag{2.63}$$

Using the same definition of I as in (2.15),

$$\dot{\psi} R_p \geq v\sqrt{\tfrac{1}{\nu}} \tag{2.64}$$

But ψ still obeys (2.3):

$$\dot{\phi} d \geq 2v\sqrt{\tfrac{1}{\nu}} \tag{2.65}$$

By simplifying the geometry in Figure 2-9, we find an approximation for the minimal approach velocity. Contact must be made exactly three quarters of a cycle after tangential near-collision at the crest.

$$a_v - v_{crit} \cdot \frac{3\pi}{2\omega_v} = 0 \tag{2.66}$$

$$v_{crit} = a_v \omega_v \cdot \frac{2}{3\pi} \tag{2.67}$$

This implies

$$\boxed{\dot{\phi}_{crit} \geq \frac{4\, a_v}{3\pi\sqrt{\nu d}}\, \omega_v} \tag{2.68}$$

If $a_v = \frac{1}{2}d$, the bolt will perforce reach 30% of its terminal velocity before it has any chance of colliding in such a way that angular velocity is subsequently reduced! Statistics will come into play for smaller amplitudes and higher speeds, but a strong bias tending to accelerate the bolt in the opposite sense of the block's motion remains. This bias only disappears at terminal velocity.

Low amplitude is necessary for (2.68) to be significant, but why high frequency? A

bolt resting in a hole is usually subject to dry friction, and enough loosening torque can only be provided at low amplitudes if frequency is correspondingly high. A generalized system is likely to face a similar constraint, but exactly what constitutes 'high' depends on application-specific details.

As stated previously, the statistical bias vanishes at steady state. This implies that even systems driven by large amplitudes could loose contact, despite existence of steady solutions to the equation of motion! Experimental evidence suggests, as reported in the next chapter, that this can indeed be the case. The expected result is a further reduction of $\tau_{d,max}$ and occasional "skipping". However, it appears that typical systems will suffer only minor performance losses under these conditions.

Chapter 3

The Experiment

As the latter sections of Chapter 2 indicate, some phenomena are best studied empirically. Others lend themselves well to mathematical modelling, but can not be fully relied upon until validated by practice. This section attempts to accomplish both ends.

3.1 Design of Experiment

Appendix A includes several views of the experimental apparatus. Inspecting these images before reading the verbal description to follow will substantially enhance comprehensibility.

A small brushed DC motor with an eccentric mass fixed to its shaft is rigidly attached to the main apparatus structure. Since the plane of rotation passes through the apparatus' center of gravity, resulting motions are exactly circular. An adjustable countermass allows precise balancing, while an accelerometer mounted vertically above the motor records vibrations. Also in the plane of rotation, a modular attachment holding a bolt or a nut may be attached.

A model S2322.980-52.235-200 DC Maxon motor, designed to operate at 9 Volts, actuates the device. A small aluminum track is press fitted to the motor shaft, with

holes spaced 3mm apart. Either a 1.1 g and a 2.2 g mass, depending on the desired range of excitation amplitudes, can slide radially along this track. A small piece of wire is inserted and bent into the track hole to safely hold the eccentric mass in place. The entire structure is waterjet-cut from sheets of 6061-T6 aluminum, a choice of process that allowed high precision and mass minimization. All connections are welded for maximum rigidity, except for those that required frequent disassembly, which are bolted. Since the apparatus is calculated to weigh about 360g, the range of attainable amplitudes can be computed from the following formula:

$$m \cdot R = M \cdot r \tag{3.1}$$

which is a direct consequence of momentum conservation for an isolated planar two-body system. This isolation is achieved through suspension from three flexible nylon strings. With the mentioned values, a range of 9 to 205 microns is possible, well below and significantly beyond a 100 micron bolt to wall separation.

The countermass constitutes 10% of the experiment's total weight, and compensates up to $\pm$ 2.4mm of vertical deviation from the digitally computed center of mass. Since the entire experiment is less than 150mm tall, this constitutes about 1.5% of the overall length in either direction.

The accelerometer is a 0.8"x0.8"x0.8" cube with frequency sensitivity beyond 10 kHz, and an output scaling factor of 100 mV/g, "g" being the acceleration due to gravity at the earth's surface.

To uncouple the constraints of balancing the experiment with different modules, the modules were designed to attach in the plane of rotation. Since both are symmetric, a balanced apparatus before module insertion guarantees a proper weight distribution afterward, as experiments may verify.

Rough calculations quickly determine that resonance is not a concern. The nut module bolt, considered the most critical element, is computed to resonate at 160 kRPM, or 2500 Hz, with the nut in the center of the structure. Since the motor frequency is limited to about 250 Hz, no noticeable resonance occurs.

3.2 Setup

Since the design is fairly flexible, a number of setups are possible, depending on the relevant experiment to be run. However, most setups involve the same measurement routine.

The first step is apparatus inspection for irregularities, such as accelerometer misorientation, loose suspension, or motor bearing failure. (The bearings are nominally overloaded by a factor of 2-6, but since the published ratings are conservative and determined for continuous operation, no problems have surfaced.) Then all necessary electrical connections are made. Specifically, the motor must be connected to a variable DC power supply, while the accelerometer linked to a four-channel data analyzer, both of which, in turn, require standard AC power. The analyzer is capable of providing time traces or frequency spectra, both of which were recorded. Subsection 3.3.1 shows sample output for the device. Sampling rate and anti-aliasing are all conveniently handled by the machine's internal software, obviating the need for Nyquist frequency computations and other sampling checks. No symptoms of aliasing or other data distortion are evident, especially since the frequencies in question are well below the device's limits.

For each data point to be collected, the relevant adjustments need be made. In most cases, only the eccentricity needs to be varied. To collect the type of data presented in Subsection 3.3.5, a light piece of non-compliant string (dental floss) is carefully hot-glued to the tip of the bolt, with special care taken to ensure that the string remains centered. A variable number of identical weights are then suspended by this string, permitting control of the payload.

With the accelerometer collecting data, motor voltage is slowly incremented until stall is observed. At that moment, the current measurement is frozen and recorded. For stall measurements, the motor is always switched to induce upward motion, with the reverse true for induced frequency measurements, which can only be performed on the nut module. In that case, the nut is manually retained at the uppermost position until the motor reaches a steady speed. Then, a digital stop watch is activated

simultaneously with the nut's release. Frequency data is frozen in mid descent, and the arrival time is recorded on the stop watch. Finally, the measured frequency spectrum is visually inspected for irregularities, and the peak frequency and amplitude recorded.

3.3 Data / Results

3.3.1 Data Collection

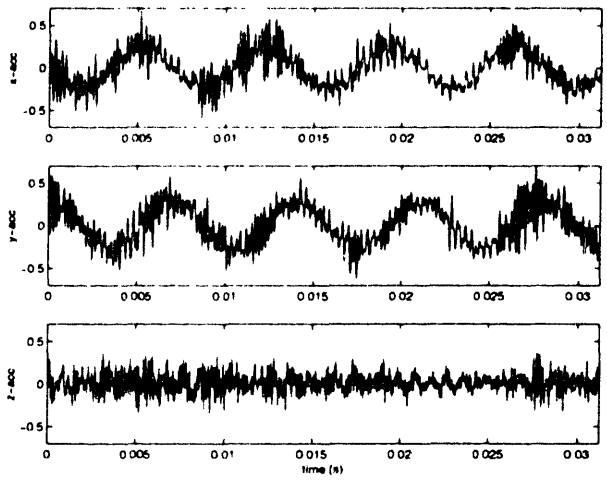

Figure 3-1: Typical time trace

Figure 3-1 captures a typical accelerometer time trace, as measured on the analyzer. x and y motions are separated by a phase very close to 90^o, while z accelerations are negligible. Although useful in discerning the proper waveform of the input, noise limits the utility of time data. The spectrum in Figure 3-2 was recorded while the nut moved along the rod. When the bolt or nut was prevented from turning, noise visibly and audibly fell.

In the frequency domain, the data is much more revealing. Frequency and amplitude can be determined with high accuracy, given a stable signal. Figure 3-2 shows the output from all three axes of the accelerometer. X and Y amplitudes are 5.4%

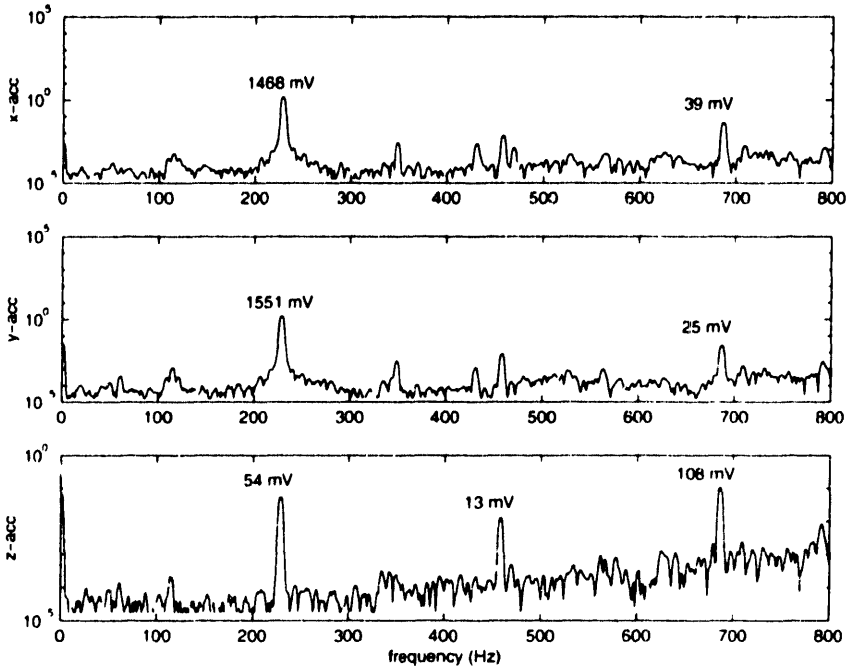

Figure 3-2: Typical frequency spectrum

apart, while Z motion is only 0.35% as strong as its counterparts. Higher order peaks are present, but benign. Displacement relates to acceleration by the square of the frequency, so high frequency peaks exaggerate the severity of the underlying cause.

Broad-band noise is clearly present, but no resonant peaks are discernible below 10 kHz (not shown). The experimental apparatus is rigid well beyond the maximum motor frequency, and undergoes circular motion to high accuracy.

3.3.2 Velocity

The kinematic relation for a nut is:

$$\dot{\psi} = -\frac{d}{D_n}\dot{\phi} \tag{3.2}$$

From an inspecting the equation of motion it is clear that if all retarding forces are overcome, the system will quickly reach steady state, in which $\dot{\phi} = \omega_v$. For

convenience, let ω_s be the screw or nut's angular speed $\dot{\psi}$ in steady state.

$$\omega_s = -\frac{d}{D_p}\omega_v \tag{3.3}$$

Later sections discuss the influence of friction and other retarding forces, so let us assume for now that the driving amplitude is sufficiently strong to induce motion.

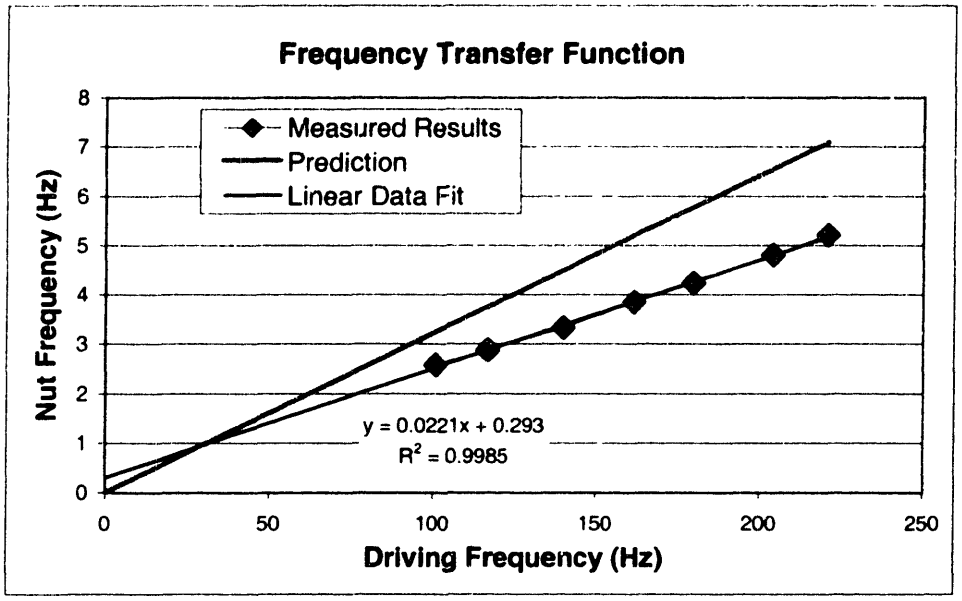

Figure 3-3: Measured relationship between forced and driving frequency

Experiments confirm the relationship between ω_s and ω_v to be astonishingly linear, as illustrated in Figure 3-3. With a correlation factor $R^2 = 0.9985$, or 0.9921 if the linear fit is forced to pass through the origin, the data nicely supports the theory.

Unfortunately, similar things can not be said about the observed slope. Assuming that we can trust the published pitch diameter of 0.220", curve fitting would suggest a gap of 4.82 thousandths of an inch, or 123 microns. With the help of a deflection gauge of approximately $0.5 - 1$ mil resolution, the gap was determined to be 7 mils. Official tolerances are too wide for guidance, allowing gaps ranging from 0 to 14 microns for a $\frac{1}{4} - 20$ nut. The discrepancy may still lie within experimental error, although 34% deviation is worth some attention. Perhaps future experiments and improved models

will be able to resolve this issue. Fortunately, the gap d does not appear prominently in the equations of motion.

3.3.3 Amplitude

Theoretically, the amplitude of oscillation should have no effect on the induced speed of rotation, once friction is overcome. In other words, basic theory predicts a step function jumping from zero to the kinematically prescribed speed at the required break-free torque.

Since this experiment demanded constant speed at varying amplitude, the power supply to the motor was set into the current limited regime. With the motor receiving a constant 225 mA, speed only dropped marginally at higher loads. To compensate for the variation, which amounted to ±6% at the extrema, measured nut speeds have been normalized by the actual frequency of excitation. The resulting data are illustrated in Figure 3-4.

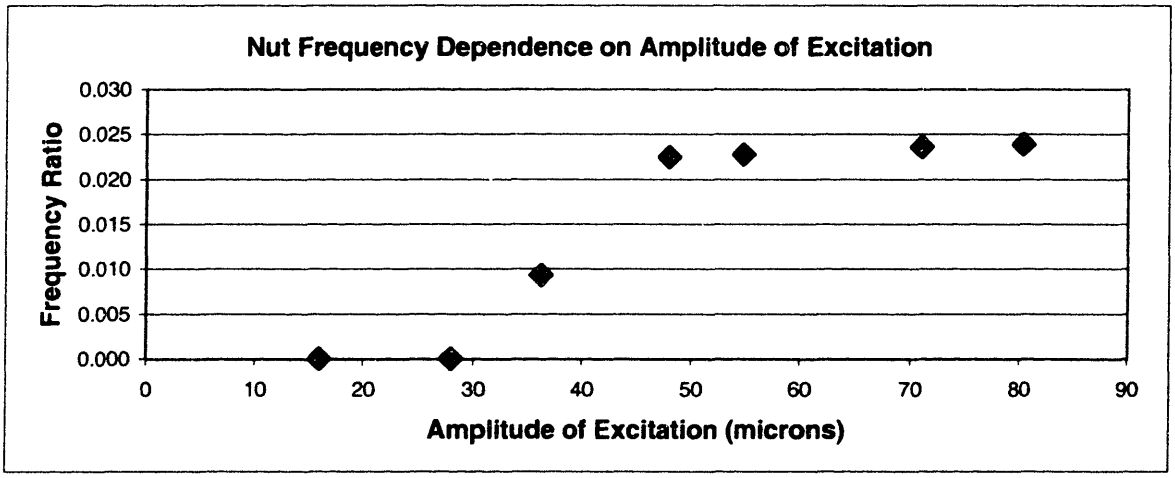

Figure 3-4: Measured relationship between forcing amplitude and nut speed

Evidently, data roughly matched the predicted results. The minimum amplitude necessary to induce motion at the motor frequency of 235 Hz is about 40 microns.

Not surprisingly, the transition to motion is not as abrupt as naïve theory would predict. Variations in the coefficient of friction, surface finish, and external distur-

bances may all contribute to a gradual transition. However, surface geometry is unlikely to vary to the degree required to explain the observed results, and external disturbances are minimal, since the nylon string constitutes a low-pass filter. It is more likely that the measured response is a complicated dynamic phenomenon, with infinitesimal disturbances providing seeds for irregularity. For practical purposes, most VIR devices should simply be designed to operate beyond the transition point.

Experimental observations provide further clues. The nut moved sporadically in the transition regime, sometimes coming briefly to a complete stop, sometimes moving visibly slower than at other times, and achieving an average speed substantially lower than the prescribed speed. At one spot about 40% from the bottom of the threaded section, the nut was more likely to slow down or stop. A barely noticeable change in friction was felt when manually turning the nut along the rod over this point, lending support to the surface disparity theory. However, the effect was far from deterministic, since the nut often traversed the section without difficulty, and other spots led to slowdowns in no predicable manner. These observations seem to indicate that higher order dynamic effects become noticeable in the transition regime. In closing, it should be noted that the perceived "roughness" was truly minor, and did not invalidate other results.

3.3.4 Stall Speed

Equation (2.48) provides an upper bound to the amount of retarding force a VIR system can sustain. Figure 3-5 shows the experimental findings, along with two theoretical curves. The lower curve represents the lowest frequency at which motion could occur, given a coefficient for unlubricated steel-on-steel of 0.8, amplified through a 30^o contact angle. The effective coefficient of friction is therefore

$$\mu_{eff} = \frac{\mu}{\cos 30^o} = 0.92 \tag{3.4}$$

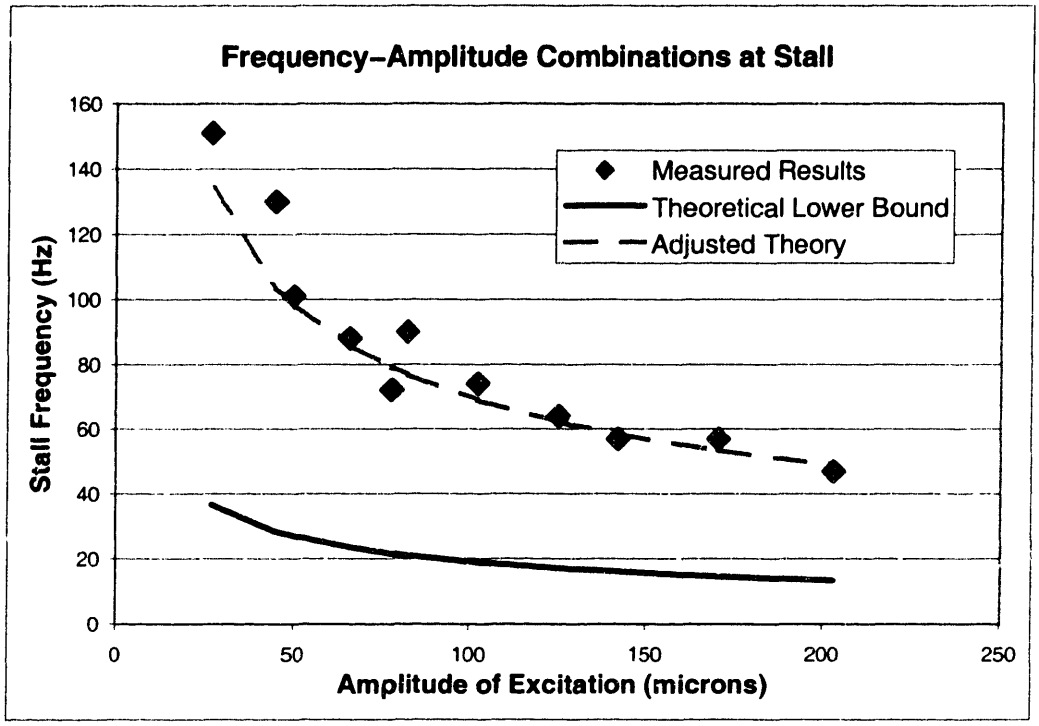

Figure 3-5: Stall frequency at various amplitudes

This prediction is clearly a lower bound, but not very satisfying for estimation purposes.

As discussed in Section 2.3, the actual load capacity has to be substantially less than that given in (2.48). The dashed curve scales the solid one, assuming a constant empirical "efficiency" of 27%. To first order, the data seems to agree with this approximation.

3.3.5 Payload

In this series of experiments, a variable weight was hung from the excited bolt. Since the string supporting the ballast has practically no torsional stiffness, and the angle of deflection is unnoticeable, the loading conditions should very closely approximate those assumed in deriving (2.48). The results are visible in Figure 3-6.

Again relying on a constant "efficiency" factor, we would expect $F \propto a_v \omega_v^2$. The

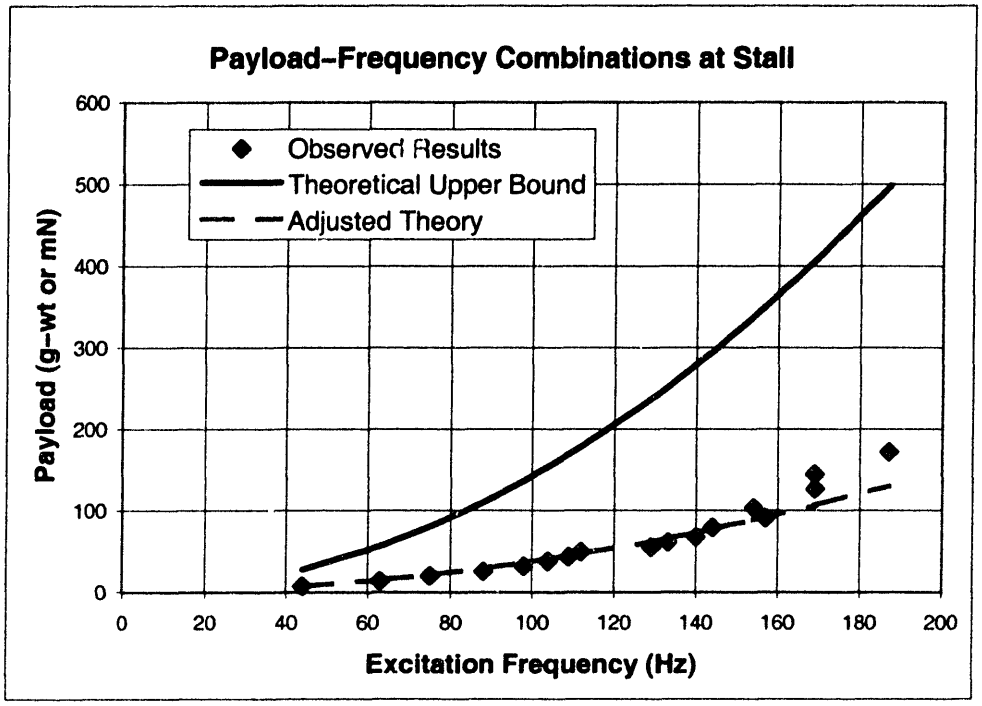

Figure 3-6: Stall payload at a given frequency

adjusted theoretical curve remains within experimental error of the observed results over a wide range of loading conditions. Since the bolt only weighs 7.3 g, the payload at 187 Hz amounts to over 23 times the driving mass!

So how valid is the constant efficiency assumption, and what efficiencies can one expect? Figure 3-7 shows computed efficiencies for various loads and three different driving amplitudes. Since the graph combines a wide range of conditions with a variety of assumptions, it appears to be rather noisy. No obvious trend is apparent, although efficiency generally tends to increase with load. In addition, one or more peaks appear to break monotonicity for medium loads.

The 41 micron amplitude data set, at 34% of the screw gap, represents low amplitude excitations. It has the most prominent peak, and values decline monotonously thereafter. Continuous curvature would suggest an eventual improvement in efficiency, but the motor was unable to provide the frequency of excitation necessary to support larger loads.

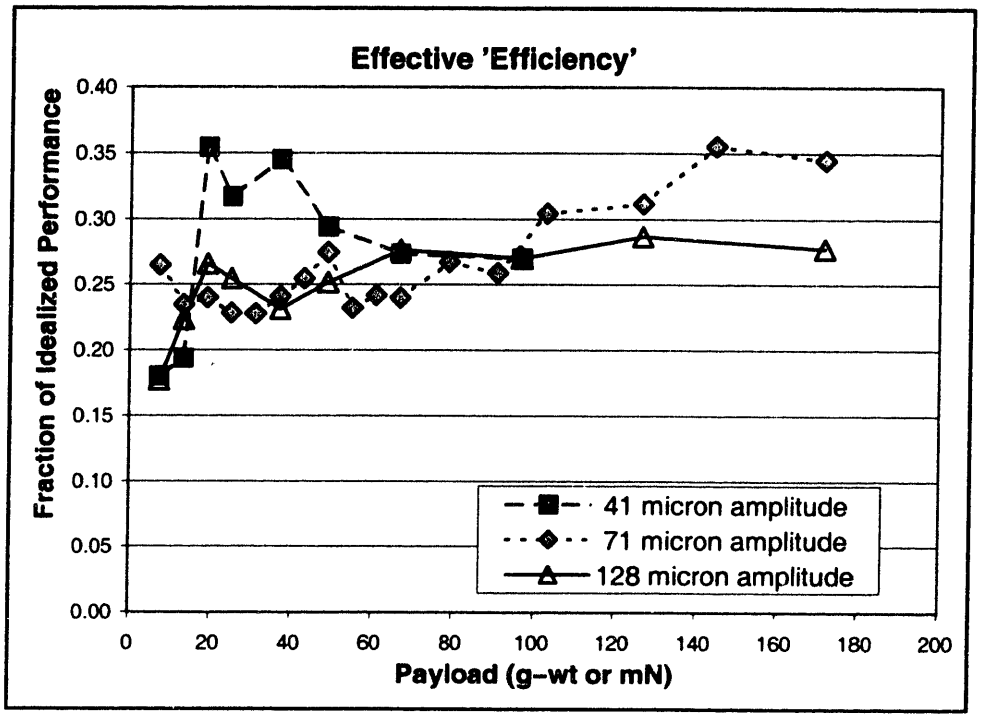

Figure 3-7: Computed efficiency under various loading conditions

A peal-to-peak excitation of 142 microns is approximately equal to the gap, half way between the interpolated 123 microns and the directly measured 178 microns of play. Its curve shows a modest peak at best, but improves steadily with load. In addition, the efficiency is unseasonably high at low loading, hinting at the possibility of multiple peaks. The large-amplitude curve resembles the intermediate amplitude one, but climbs less steeply. Relatively speaking, it is not clear what effect amplitude has on efficiency.

Collecting the data for Figure 3-7 was difficult, especially at very high frequencies or low amplitudes. The standard deviation of frequency at stall reached 6% under some conditions, improved noticeably for larger loads, and declined again at the high end. For large loads, hysteresis made data collection particularly difficult. A bolt would not move for several seconds, and suddenly, despite any change in motor voltage, climb steadily upward. Large numbers of repetitions were avoided at these amplitudes to prevent deterioration of the overloaded motor bearings.

Despite the aforementioned difficulties, the peaks appear to be statistically significant. It should also be noted that the bolt shows no signs of stalling once motion commences, providing strong evidence that the maximum starting torque is substantially lower than the maximum stall torque, a very intuitive result. Yet without further modelling and more elaborate experimentation, any more speculation is futile. The given inferences are already somewhat risqué, included here not as a statement of fact but to provide guidance and foresee potential problems for future experimenters.

3.3.6 Orientation

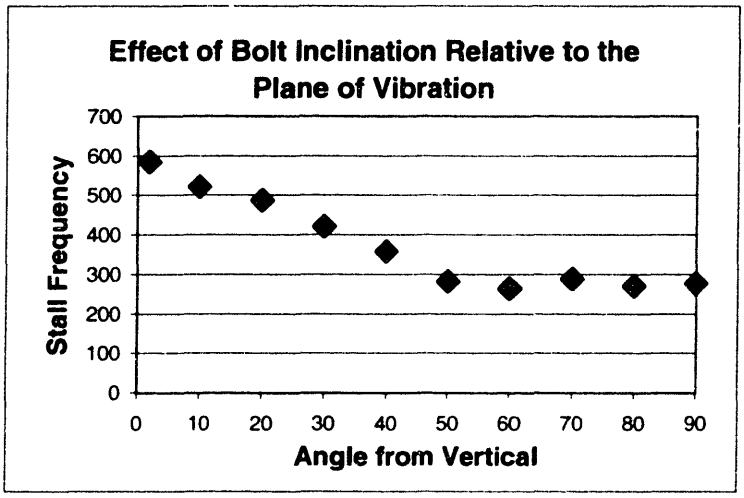

Figure 3-8: Effect of misorientation on break-free amplitude

This subsection is by necessity very empirical, since the experimental apparatus is not explicitly designed to examine the question of misorientation. The internally threaded module could be tilted to varying degrees, but too many things change at once to allow a clean analytical model. As the angle between the bolt axis and the normal to the plane of rotation is varied, the bolt is subject to intense axial excitation, and its orientation relative to gravity changes as well Nevertheless, the experiment remains worthwhile, since it explores a set of conditions that are likely to be present, or potentially present, in a variety of applications.

In Figure 3-8, we see that bolts will still turn — even at orientations approaching tangency to the rotation plane. There is no gradual increase in the amount of force required, culminating in complete lack of motion at small angles. In fact, it was practically impossible to find an orientation in which the bolt did not move one way or the other. One component of excitation is enough to provide the energy to move the bolt, especially when z-motion is effectively reducing friction, while the other component need only provide sufficient force to induce a directional preference.

3.3.7 Partial Insertion

During all preceding experiments, care was taken to ensure that the bolt was centered and contacting the block over most of its threaded section. For various reasons, applications may not meet these conditions. Quantification of these effects would provide enough work for several studies, but the following observations, based on work done on a long bolt, should provide a general idea of what such studies might find.

Surprisingly, VIR tends to remain in effect over almost the entire range of motion. At high frequencies, the bolt wound its way up the block, slowed down at the last thread, but continued until falling out of the hole. At 55 Hz, only slightly above stall speed, the bolt began to slow down much earlier, but steadily unwound almost all the way, stopping with about 25^o degrees of thread remaining.

Starting from the unthreaded state was just as easy. At 52 Hz, after a wobbly start, the bolt proceeded to engage. After several turns, motion became erratic, loud, and inefficient, indications that collision-dominated motion similar to that discussed in Section 2.5 was in effect. Chatter abruptly stopped the moment the tip of the bolt emerged from the threaded section, with surprising repeatability. This observation suggests that a more complete three-dimensional model may assume contact at the first and last threads in contact only.

At higher speeds, starting became progressively easier. Even at the maximum speed of 230 Hz, it was clear that a bolt, once engaged, reliably continued to screw

its way into the block. And as long as the bolt was held in an orientation reasonably close to normal to the surface, it bounced, turned, and engaged without fail.

As a bolt is driven further into the block, the distance of its center of mass to the hole's axis of symmetry will vary. Effectively speaking, the gap d changes, which should result in *higher* speeds. This was observed briefly for an ascending bolt, but a descending one did not reach the proper configuration. It appears that driving amplitudes much smaller than the gap do not tend to lead to the stable, steady motions assumed in most of the theoretical section of this thesis. When the bolt shaft was manually steadied by slight contact, rattle ceased immediately, and the bolt instantly turned many times faster. Finally, there was evidence for an unstable zero-speed mode, in which the center of mass remains exactly on the hole axis, while the bolt head and tip counterbalance each other. As the long bolt slowly engaged, it often remained in place at what appeared to be the right position, but quickly transitioned to larger amplitude head motions. Future studies should consider the use of high speed video imaging to observe and confirm different modes of motion.

Chapter 4

Conclusions

4.1 Applications

4.1.1 Conventional Fastener Assembly

VIR is ideal for reducing fastener insertion time, especially when several bolts need to be assembled in parallel. Unfortunately, without any further innovation, both theory and experiment suggest that VIR is unlikely to sufficiently tighten a bolt or nut for conventional assemblies. Subsection 4.1.3 will discuss several approaches to this problem. Nevertheless, VIR can be economical on the basis of faster insertion alone.

In the context of high volume automated production, VIR offers many advantages. Parallel insertion capability is the main economical driving force, since any number of bolts of arbitrary style and size can be inserted at once. Section 3.3.6 reports that VIR performance drops off very little at steep angles, which implies that a single fixed rotating imbalance could easily be used for bolts that are on orthogonal faces. In fact, almost any bolt in any orientation can be serviced by a single source of vibration, as long as the bolt axis is beyond 10^o degrees from the rotation plane. This means that bolts on three orthogonal faces of a cube-shaped workpiece could all turn at once,

with an angle of attack of 35.26^o degrees. Geometry in fact assures the existence of an orientation that spins all bolts in the proper direction in this case, if all sides are equally accessible.

Since torquing in different planes would usually require either multiple robots or a significant transition time, the motor could be stopped and reversed at the proper time, with the initial bolts held in place by their pre-load. Care should be taken to ensure that the second phase of insertion does not loosen the first batch of bolts, although quality constraints should already preclude such an occurrence.

An engineer wishing to implement VIR has the luxury of choosing the amplitude, frequency, and angle of attack independently. Since the angle of attack only has a weak effect, it should be determined by the most convenient fixturing method. Frequency and amplitude are subjected to the minimum torque relation, which derives directly from (2.47):

$$a_v \omega_v^2 \geq C_{Empirical} \tag{4.1}$$

Finally, the frequency should be chosen in a regime that does not excite the workpiece's resonant modes, while the amplitude of excitation should be on the order of the screw gap. In difficult cases, it may be worthwhile to change the amount of play in the screw.

Heavy workpieces can easily require unusually large bearing forces, if the source of excitation is indeed a motor equipped with an eccentric mass. Unfortunately, (4.1) also implies a constant radial bearing load, assuming that the degree of eccentricity is adjusted to produce the proper amplitude at a chosen frequency. However, clever engineering can reduce demands on the actuator. The workpiece only has to oscillate locally, so compliance or even resonance could be exploited. At the least, the workpiece can be excited in such a way that center of mass motion is minimized, with rotations about the center of mass providing all the motion.

The potential advantages of such a system grow with the degree of integration with the manufacturing and even design processes. In the extreme case of an existing assembly line, VIR could be brought in to eliminate problem areas. In the

production-line planning phase, VIR should be able to reduce the number of stations required, requiring fewer torquing robots (reducing fixed and maintenance costs) and permitting faster throughput. The design for the remaining robots could be simplified as well, since they would no longer be required to produce high torques *and* high speeds. Furthermore, reliance on VIR could allow greater freedom to the product design engineer, who faces an expanded production possibility frontier. In addition, the design engineer can tweak the product to maximize VIR effectiveness, e.g., by introducing selective compliance mentioned previously. Introducing VIR on higher levels of the production hierarchy implies longer and increasingly elaborate learning processes, but promises greater long-term rewards.

Low or medium volume production, involving manual bolt tightening, faces very similar tradeoffs. Here, the flexibility of VIR should prove to be most advantageous. A rapidly evolving design should not entail elaborate fixturing changes, in most cases. A simple vibration inducer may be economical long before full automation is, and may remain useful, with minor modifications, for future product lines.

4.1.2 Tool for Specialized Professionals

Mechanics, Jewellers, and other professionals alike could potentially benefit from a VIR device. Although it may seem unlikely, at first glance, that VIR could augment the conventional power screwdriver, several niches exist. These include:

Inaccessible Locations: A bolt or nut may be in an area that is difficult to access with conventional tools.

Damaged Set Screws: VIR does not require direct contact, so stripped set screws could be actuated as easily as new ones, barring mechanical jamming.

Small Screws: Watches and other jewelry often make use of # 2 screws and smaller. It may be easier to clamp a vibration inducer to the watch than to find the slot in the screw head.

Automation: For large arrays of screws, bolts, or nuts, VIR may prove to be an actual time saver.

Pre-tightening: In systems with a high degree of compliance, VIR could ensure constant and equal pre-tightening of the relevant screws. For example, a gasketed system could be pre-loaded to the desired amount, abating the problem of equalizing pressure.

An affordable VIR tool could prove useful in a myriad of unforeseeable situations.

4.1.3 Novel Tightening Methods

Despite all advantages mentioned in Subsection 4.1.1,the potential of VIR is constrained by its reliance on other torquing mechanisms. No obvious general solution is apparent at this time, but further development could break this barrier. The following approaches may prove more or less generally applicable. Hopefully breakthroughs will be motivated by immediate needs, but extended, once successful, to broader areas.

Thermal Tightening

In conventional thermal tightening, a bolt is heated after insertion, the head indexed through a prescribed angle, and the bolt allowed to procure its own preload during thermal contraction. The procedure is applied to large structural bolts, whose preloads are too immense to provide with standard pneumatic or manual wrenches. Torquing inaccuracy and complexity have limited the use of thermal tightening as a production process.

VIR would provide the perfect complement to thermal tightening, since one can insert and the other torque the bolt. The required thermal gradients are not as large as one might imagine. Let ΔT_y be the minimum temperature change capable of creating plastic deformations. Then from an elementary force balance

$$\alpha \Delta T = \varepsilon_{thermal} = \frac{\sigma}{E} \tag{4.2}$$

we find

$$\Delta T_y \equiv \frac{\sigma_y}{E\alpha} \tag{4.3}$$

The yield temperature is a derived material property. For a strong steel with $\sigma_y = 400MPa$, $E = 210GPa$, and $\alpha = 12ppm/K$, T_y is only 159°C! Aluminum alloys vary widely in their properties, but 6061-T6 is comparable at 164°C, with most alloys yielding sooner.

Although bolts are usually tightened to only 80% of their yield stress, a number of factors would require heating to much higher temperatures. Joint compliance will scale the requirement by the joint constant, which, at typical values around 2.0, should not prove fatal to the idea. However, the bolt will cool quickly, especially under the influence of vibration-induced convection, and bolt speeds are limited by the actuator's performance.

The supreme challenge in such a procedure seems to be process control. Minute initial gaps between the two media to be joined, or the upper medium and the bolt head, can remove preload entirely. The process is equally sensitive to uneven cooling rates. Nevertheless, the idea is not infeasible *per se*, and successful implementation could eventually prove lucrative.

Pre-preloading

Some systems do not require a large preload, or are intended to remain partially compliant by design. Most gasketed joints should fall in this classification. In such cases, combining VIR with mechanical preloading of the joint may be sufficient to ensure a satisfactory connection. Although this process is quite feasible, its domain appears to be limited.

Inertial Tightening

If a bolt gained enough momentum during its descent, it could theoretically transform enough of this energy into elastic deformation of the joint and bolt shaft. Such an

approach would probably require ultrasonic excitation frequencies, although amplitudes need not be that high. A model capturing all the dynamics of starting a bolt would be necessary for a fully informed judgement, but present evidence suggests that inertial tightening would be difficult at best.

4.1.4 Fastener Production

VIR devices might prove particularly useful in the production of threaded fasteners. Production methods vary widely, and no attempt has been made to study them extensively. However, fastener producers should examine their current processes, and consider augmenting them with VIR. VIR provides a method of handling bolts through circumferential contact, which may permit less cooling between stages of production, and conceivably help ensure thread uniformity and surface finish.

Equation (2.3) suggests a simple yet accurate procedure of measuring adherence to pitch diameter tolerance, and VIR could even be used to mechanically sort bolts by gap size. Similarly, (2.47) implies a means of measuring surface roughness and disparities, a potential concern in high quality applications.

4.1.5 Fastener Loosening

Considering the ubiquitous presence of threaded fasteners, it is not surprising that many investigations have been performed to analyze fastener loosening. The novelty of VIR derives from the idea of harnessing loosening mechanisms to one's benefit, inverting the problem into a solution. Still, this study provides some insights into the original problem that should not be overlooked.

Mechanism of Loosening?

If VIR is a mechanism of fastener loosening, it has never been rigorously examined as such. Studies claim that unidirectional excitations normal to a bolt shaft provide the most potent means of vibrational loosening. It does not appear that two orthogonal

phase-shifted excitations were ever considered. Although such a mode of loosening might not be termed VIR in the strictest sense of the word, it does seem likely that orthogonal excitation would loosen bolts more quickly than uniaxial motion. Since VIR continues to remain effective at steep angles of attack, the observed mode of loosening would be closely related to a conceptually VIR-based mechanism.

In-line or Field Quality Testing

The ærospace industry routinely invests significant sums of money inspecting bolts for tightness, while some production lines monitor the quality of threaded joints. A small hand-held vibration inducer could potentially simplify the inspector's task. VIR may not be able to measure the degree of preload, but finger tight nuts or bolts would conspicuously reveal their defect immediately.

Fastener Design Testing

As new "vibration proof" or vibration resistant fasteners are developed, their performance must be gauged for evaluation and comparison. The *de facto* standard appears to be resistance to tangential vibration. Whether VIR is a potent mechanism of loosening or not, the introduction of a directional preference could improve, if not accelerate, looseness testing. Section 3.3.6 suggests that uniaxial vibration may be measured to be misleadingly benign, since the introduction of a slight rotational asymmetry should coordinate all a bolt's motions toward a single direction. Even if VIR were not to come into effect until a bolt is completely loose, it would at least provide a clear and unambiguous measure marking the onset of such a state.

4.1.6 Actuation

VIR presents some unique features that could make it suitable for specialized actuation. The most salient feature is the potential for large frequency reductions, which derives from the transmission ratio. Current piezoelectric actuators in camera zooms,

printer paper feeds, and other devices rely on relatively sophisticated microstructures, while a cylinder excited in a reamed hole could potentially achieve the same results. Without inherent complexity, VIR-based actuators could conceivably provide any rotational, linear, or helical motion imaginable. Linear or steep helical elements might require a de-coupling stage, depending on the implementation. A primarily rotating element could push or pull a prismatically guided member, for example.

VIR, by virtue of its simplicity, could prove useful to MEMS devices. Since piezoelectric elements are most efficient at high frequencies, the $\frac{d}{D_p}$ frequency reduction could enable high power densities. The production of useable microscopic threaded rods with uniform gap thickness appears to be the main hurdle to such a project. However, this hurdle does not seem insurmountable. One promising approach could involve rolling the threads into thin strands of wire, and testing the quality with methods discussed in Section 4.1.4. Standards could be stringent, since microscopic scales imply little volumetric waste. Internal threads would probably be more problematic to produce, but VIR only requires contact over two threads. Internally threaded end caps would therefore suffice.

Once produced, a VIR MEMS actuator provides several advantages. As mentioned, efficiency could surpass that of conventional devices. The 'efficiency' mentioned in Subsection 3.3.5 should not be confused with mechanical efficiency. Even though extremely high frequencies would probably imply collision-dominated motion, which results in forces much smaller than (2.48) would predict, output power is still input power less power dissipated. In other words, less 'efficient' motion would inherently reduce loads on the excitation device, unless it also entailed higher friction and dissipation. There is no fundamental reason why VIR devices should waste mechanical energy.

A further advantage is a practically unlimited stroke. As long as the driven rod does not buckle or adversely resonate, a VIR MEM actuator could provide force over a wide range of motion, a typical shortcoming of conventional devices.

Finally, VIR is easily scalable to an array of parallel actuators. A single block could drive an unlimited number of rods, if the application should demand such a

feature. Perhaps independent control could be achieved through individual jamming, which a small displacement of the end caps could accomplish - this is just one conceptualization of an endless array of possibilities.

4.1.7 Moving the Inaccessible

As alluded to in the discussion of fastener production and other sections, VIR provides a method of inducing motion remotely. Although no concrete application comes to mind, a number of reasons could make remote actuation desirable. The actuated object could be chemically contaminated, mechanically inaccessible, too small to handle, or too brittle to subject to tensile forces, just to name a few. Along these same lines, a moderately cohesive powder could be transported through internally threaded vibrating tubes, a system inherently resilient to clogging. Such powder might range from hydrogen pellets in fuel cells to aggressive powders used in 3D printing.

4.1.8 Ideas Requiring Extensive Further Development

Locomotion

Conceivably, the source of excitation could be internal to the threaded cylinder. Such an arrangement might be useful for a medical endoscopic robot, although it has yet to be determined if VIR would function in a liquid medium. Similar modes of locomotion could be beneficial for larger devices, such as a space probe intended to explore the interior of one of the planets in our solar system.

Display

With an array of miniature rotating rods, a flicker-free display could be created. This would require rough angular position control, which a cross-blocking member could provide. The heads of the rods would have to be equipped with disks or polygons that selectively block fractions of each other. Finding a suitable geometric arrangement

is encumbered by the constraint of finite rod diameters. Since a rod must support each disk, even a staggered configuration would be plagued by interference. Magnetic coupling between alternating members could be one approach.

Black and white displays would only require two visible states, but full color would need four. Therefore, three quarters of the surface area of every disk would have to be covered at any moment in time. Physical realization would be difficult.

Another arrangement could involve color patches on the sides of cylinders. The supporting ends would have to be thin, since they would again tend to interfere or obstruct neighboring pixels. Either arrangement is liable to be delicate and expensive, but LCD screens had a similar beginning.

Finally, an array of rods could be used to create a topological map. If equipped with LEDs or optical fibers, for example, a sophisticated depth-enhanced screen could be created. Directly retracting or extending the rods may seem like a more logical alternative at first glance, but driving the rods with VIR could, under certain circumstances, be a rational alternative. And as mentioned before, via a de-coupling element, VIR MEMS actuators may be the most promising way of effecting selective massively parallel linear motion.

4.2 Recommendations for Future Research

Vibration-Induced Rotation has just been formally discovered, and as this chapter should convey, much remains to be done. Practically every aspect could be explored and modelled in more detail.

Since this thesis has hopefully establishes a foundation on which to build, further research should be application-oriented. Any given field should come with one or more salient questions, so research should be focused along those guidelines.

In general, the most useful advancement of knowledge would arise from the development of a complete three-dimensional dynamic model, one that could predict 'efficiency', entry and exit behavior, and responses under a wide variety of conditions.

Since such a model will be complex, difficult, and potentially sensitive to disturbances, it would have to be complemented with sophisticated physical research. High speed imaging would be an invaluable tool, along with bolt-mounted accelerometers and precise three-dimensional control of the excitation. An oversized "bolt" or lead screw may also prove more convenient to work with.

Although a generalized model would be beneficial, more incremental progress along application-driven lines may prove just as useful. Specific advice, where applicable, should be in the relevant section of this document. Yet whatever line is to be pursued, loss of generality should be avoided, since broad insights are likely to yield unexpected benefits, especially in the unexplored field of VIR.

4.3 Summary

Vibration-Induced Rotation is a newly discovered mechanical mechanism by which threaded objects can be actuated. Both externally threaded bodies, such as bolts, and internally threaded ones, such as nuts, respond similarly to circular excitations. Bolts rotate counter to the sense of vibration, at a frequency that scales to the driving frequency by the ratio of the gap to the pitch diameter. Nuts obey the same equation, but turn synchronously with the forcing motion.

The linear frequency relationship described in the previous paragraph is valid for all driving amplitudes sufficient to overcome retarding forces. Quantitatively, the amount of force a body can overcome is proportional to its mass, the amplitude of excitation, the square of the frequency, a friction-related term, and a dynamic efficiency factor. A number of considerations confirm the stability and impetus toward reaching the identified steady state motions. Nonetheless, collision-dominated phases may exist during startup, and some conditions may even lead to continuous erratic motion. While the steady state modes predicted analytically are experimentally confirmed, more complicated responses are the result of empirical observations and await theoretical rigorization.

Empirical results show that VIR remains effective when the normal vector of the plane of rotation is inclined over 80 degrees from the driven body's axis of symmetry. It is sufficient for one axis to provide kinetic energy, while the other induces little more than a directional preference. VIR is also robust to minimal thread contact. At speeds barely sufficient to move a bolt in its fully inserted state, that same bolt can be driven within a quarter rotation of complete disengagement. Similarly, starting is also reliable, albeit slow, at similar speeds.

These and other results contribute encouragingly to the prospect of developing practical uses. Imbued with minimal inherent complexity, most applications will be economically competitive. Insertion of bolts, nuts, or other threaded fasteners in a production environment is the most obvious, and certainly a feasible, possibility. Unfortunately, VIR appears incapable of providing significant torquing power, so fasteners would require subsequent tightening by another method. The previous chapter suggests a number of approaches in which this problem may be overcome. Fastener looseness testing devices, piezoelectric actuators, material handling systems, and topological displays provide just a sample of the variety of avenues of further possible development. If backed by commercial interest and support, VIR could improve a variety of existing processes, but also enable solutions to challenging problems that would remain insoluble otherwise.

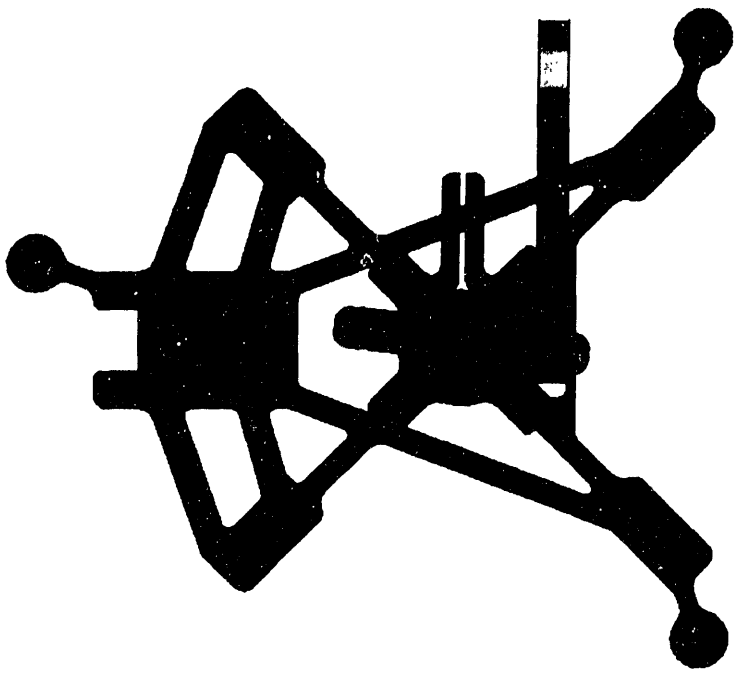

Figure A-2: Top view

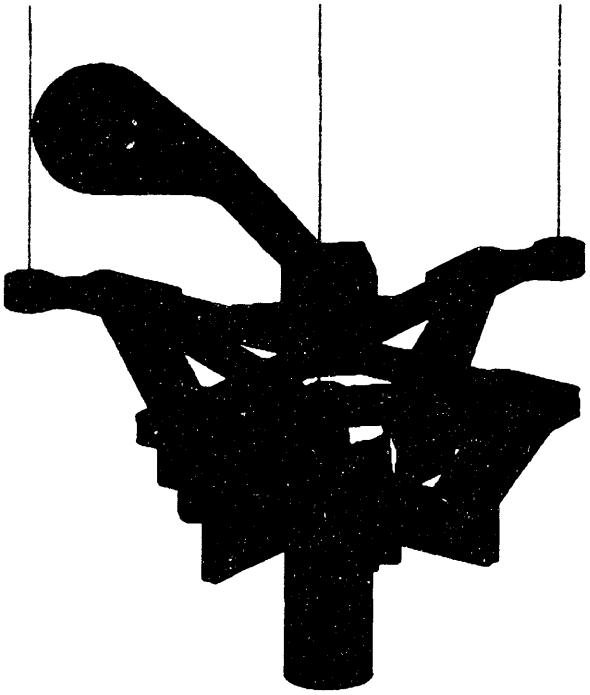

Figure A-3: Front view

Appendix A

CAD Images

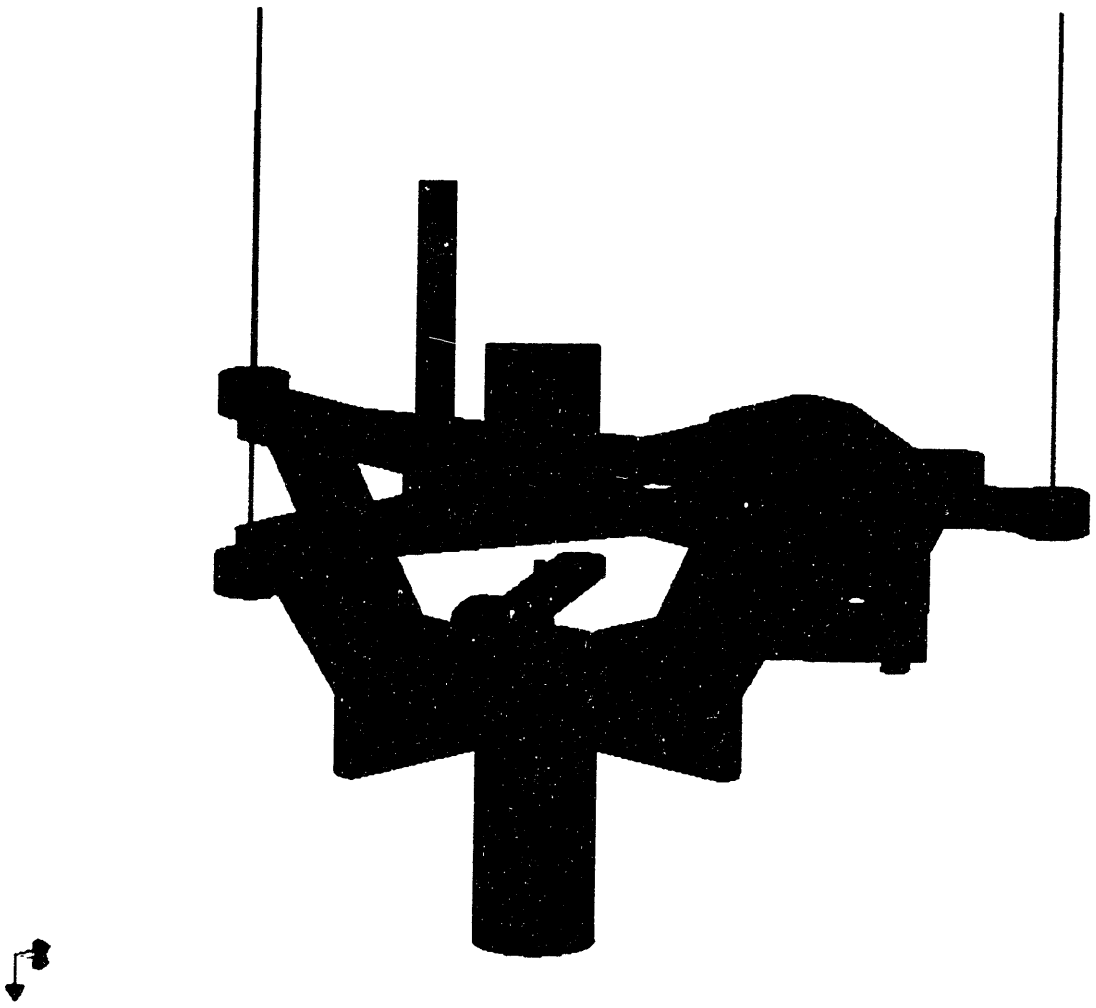

Figure A-1: Side view

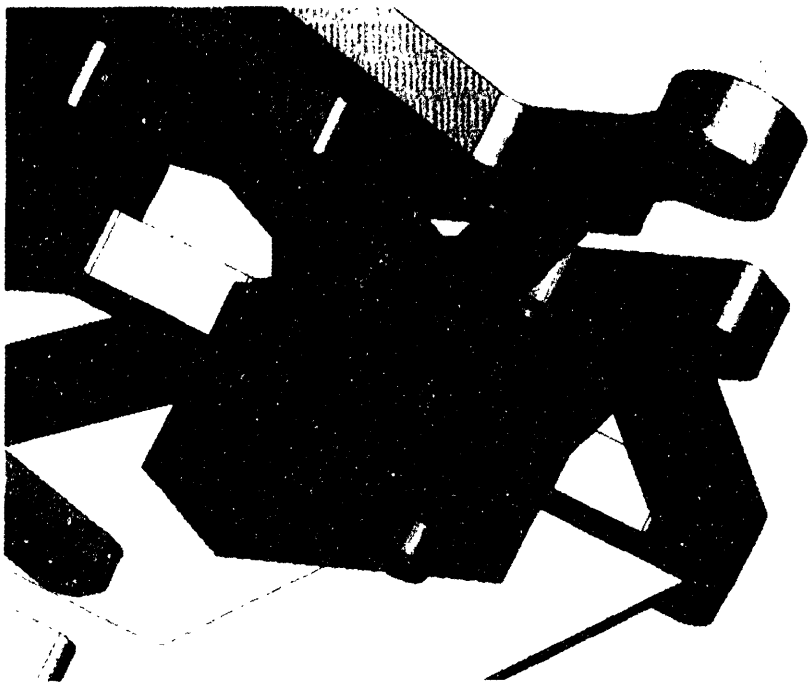

Figure A-4: Bolt module

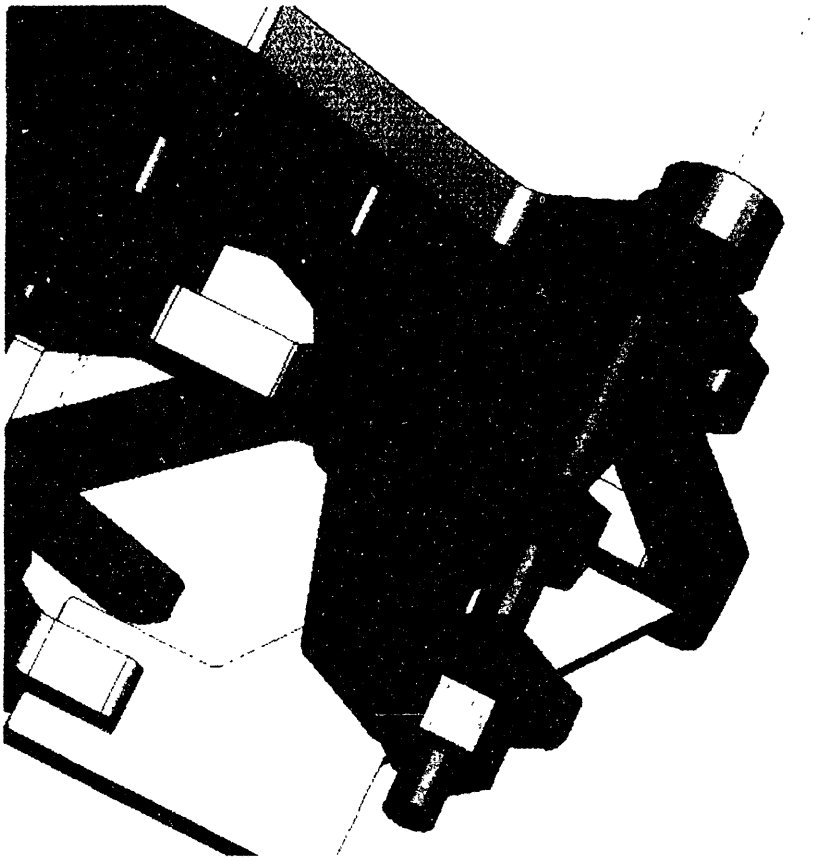

Figure A-5: Nut module